TBK1 controls IgA class switching by negatively regulating noncanonical NF-κB signaling

Jin Jin[1], Yichuan Xiao[1], Jae-Hoon Chang[1], Jiayi Yu[1], Hongbo Hu[1], Robyn Starr[3], George C. Brittain[1], Mikyoung Chang[1], Xuhong Cheng[1] & Shao-Cong Sun[1, 2]

[1]Department of Immunology, The University of Texas MD Anderson Cancer Center, 7455 Fannin Street, Box 902, Houston TX 77030, USA; [2]The University of Texas Graduate School of Biomedical Sciences at Houston, Houston, Texas 77030, USA; [3]St. Vincent's Institute, 41 Victoria Parade, Fitzroy, Victoria 3065, Australia.

Correspondence should be addressed to S.-C. S. (ssun@mdanderson.org).

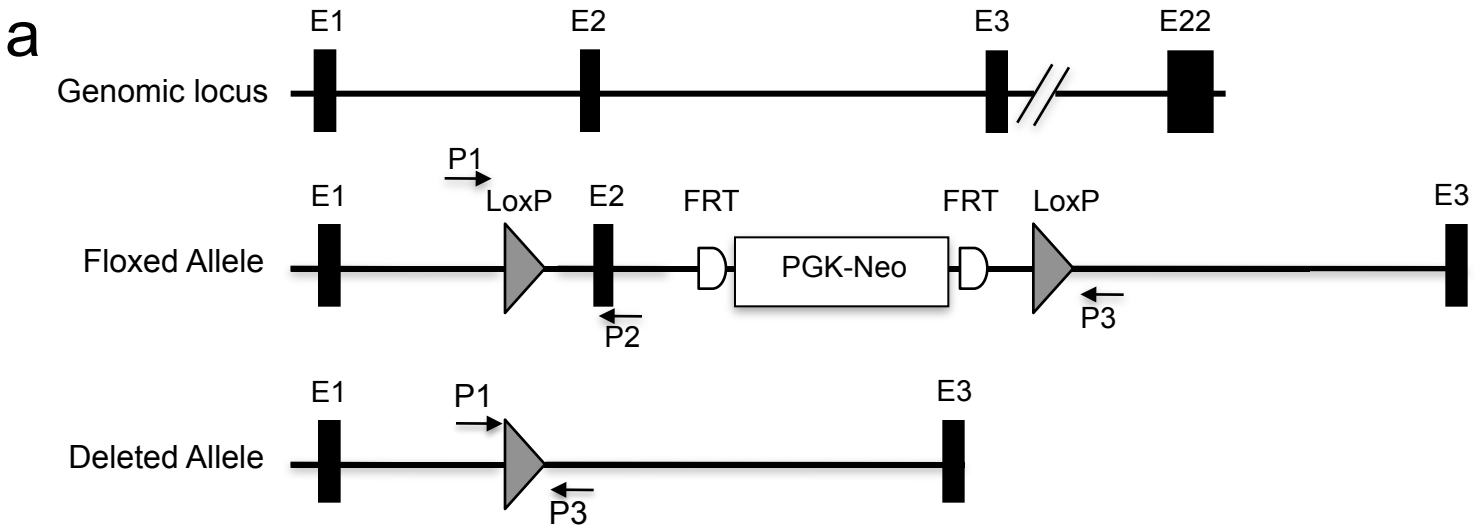

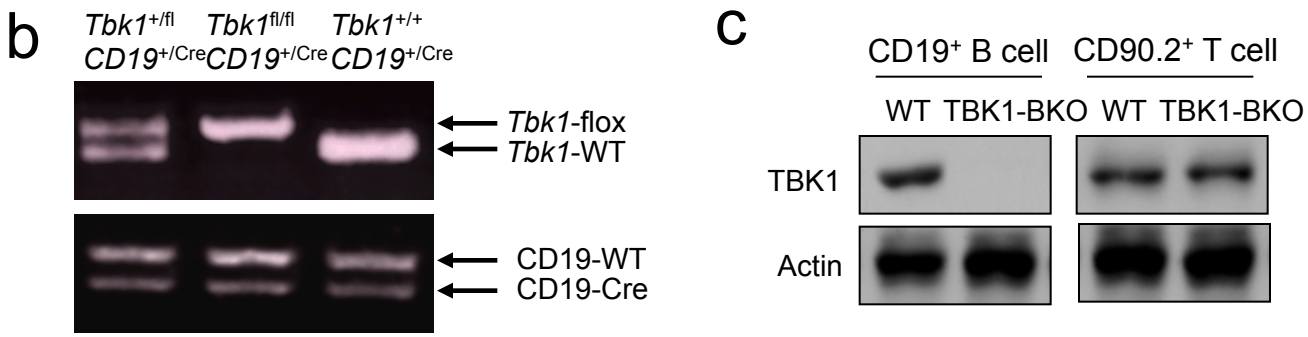

Supplementary Figure 1. *Tbk1* gene targeting. (**a**) Schematic picture showing the *Tbk1* gene targeting strategy. Floxed allele contains two LoxP sites and a PGK-neomycin cassette (flanked by two FRT sites) inserted besides coding exon 2. Deleted allele indicates the deletion of exon 2 following Cre-mediated LoxP recombination. Genotyping primers are indicated. (**b**) TBK1-BKO genotyping PCR. *Tbk1*-floxed mice were crossed with CD19-Cre mice to generate $Tbk1^{fl/fl}CD19^{Cre/+}$ (named TBK1-BKO), $Tbk1^{+/+}CD19^{Cre/+}$ (named WT), and $Tbk1^{+/fl}CD19^{Cre/+}$ mice. PCR was performed to detect the WT and floxed *Tbk1* alleles (with P1 and P2 primers) and to detect the WT and Cre-expressing CD19 alleles (following Jackson Lab protocol). (**c**) Immunoblotting assays showing specific ablation of *Tbk1* in the B cells of TBK1-BKO mice.

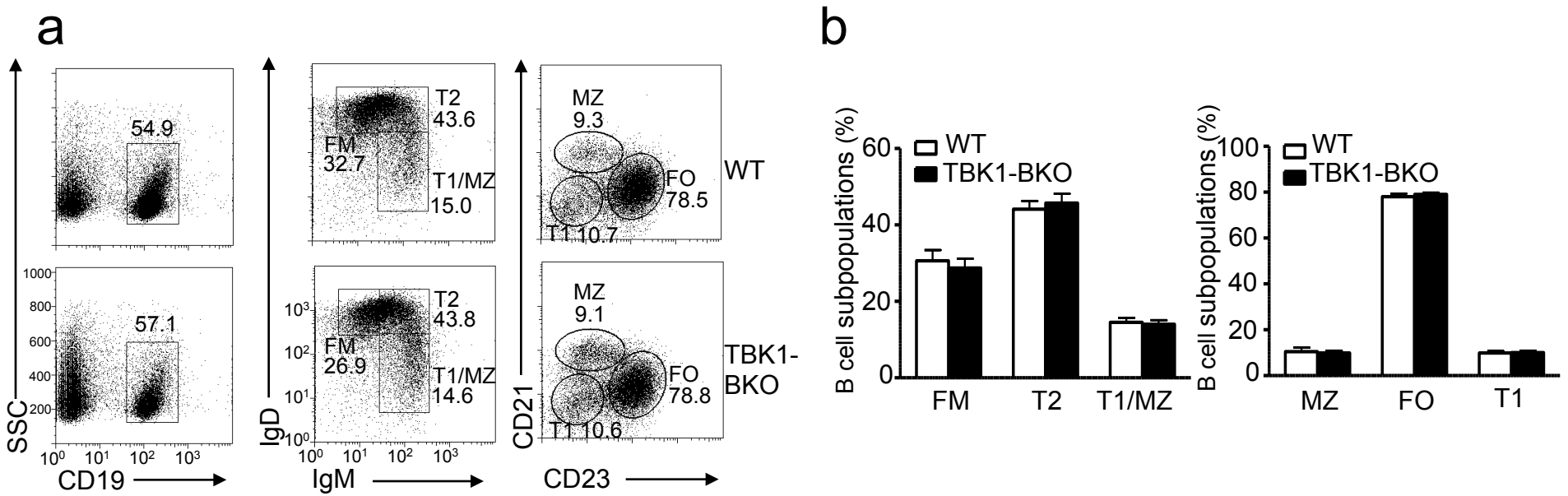

Supplementary Figure 2. B-cell conditional Tbk1 gene ablation does not affect B-cell maturation in the spleen. (**a**) Flow cytomery measuring the percentage (numbers in quadrants) of B-cell populations among the $CD19^{+}$ splenic cells in the spleen of WT and TBK1-BKO mice ((6 weeks of age). (**b**) Summary of **a**, showing the mean ± S.D. values. FM, follicular mature ($IgM^{int}IgD^{high}$); FO, follicular ($CD21^{int}CD23^{high}$); T1, transitional 1 ($IgM^{high}IgD^{low}$, $CD21^{low}CD23^{low}$); T2, transitional 2 ($IgM^{high}IgD^{high}$); MZ, marginal zone ($IgM^{high}IgD^{low}$, $CD21^{high}CD23^{low}$). Data are representative of 6 animals in two independent experiments.

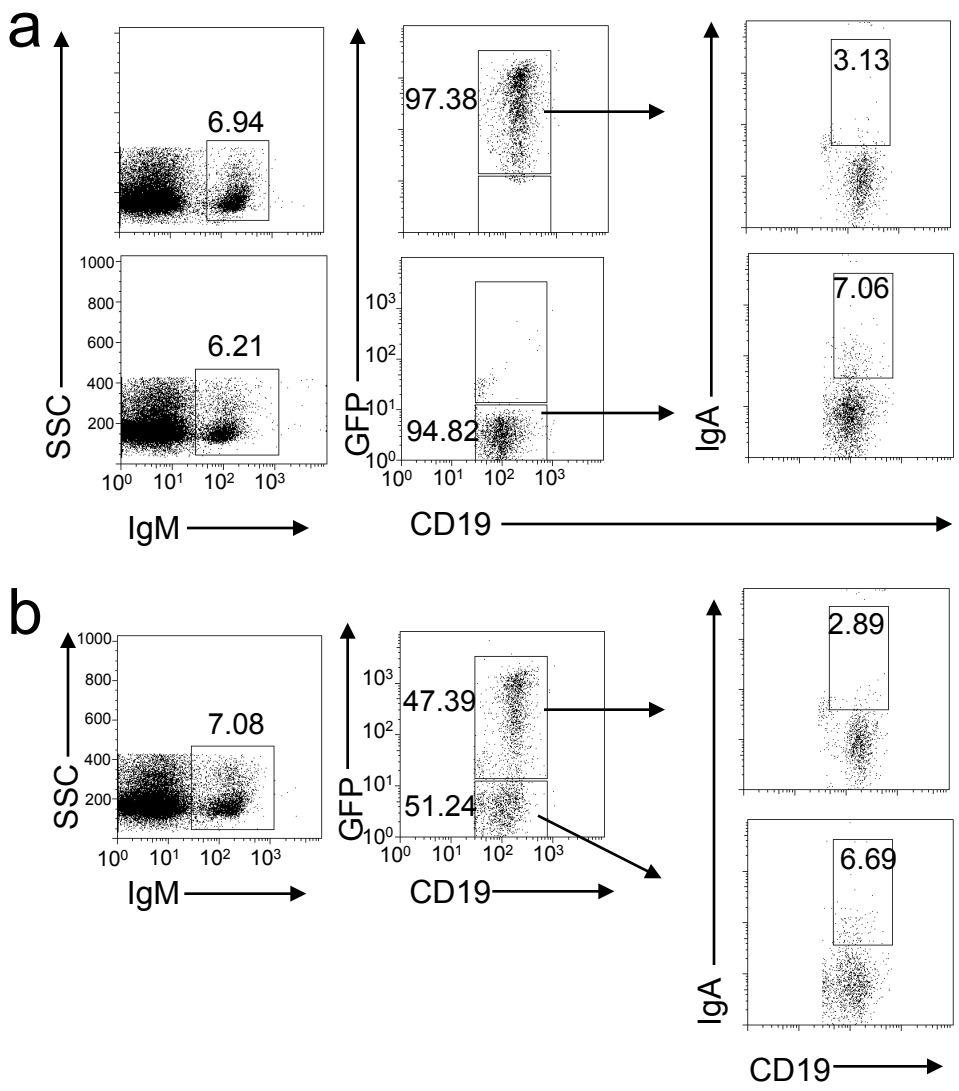

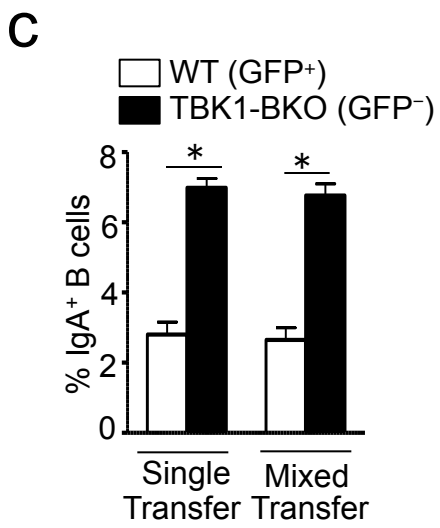

Supplementary Figure 3. B-cell intrinsic function of TBK1 in the regulation of IgA production. (**a-c**) The IgM KO mice (lacking mature B cells) were adoptively transferred with IgM$^+$ splenic B cells (1×10^7) purified from GFP-expressing wild-type mice (WT, GFP$^+$) or GFP-negative TBK1-BKO (GFP$^-$) mice (6 week old) (**a**) or a 1:1 mixture of GFP$^+$ WT B cells and GFP$^-$ TBK1-BKO B cells (**b**). Recipient mice were immunized i.p. with sheep red blood cells (SRBC) and sacrificed on day 7. The frequency IgA$^+$ B cells in the gated GFP$^+$ or GFP$^-$ splenic B-cell populations was quantified by flow cytometry and presented as a representative plot (**a, b**) and summary graph (**c**). *P<0.05.

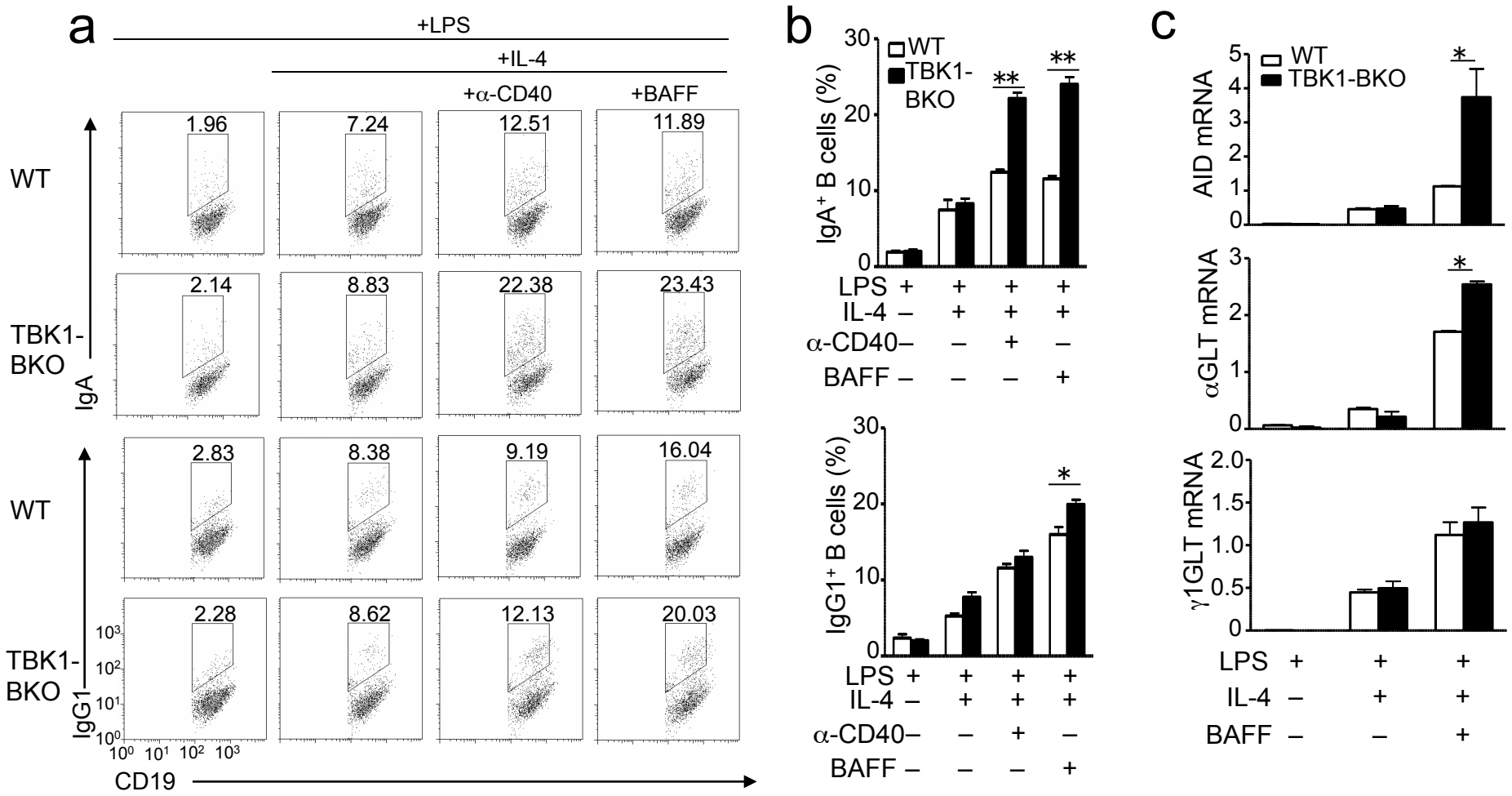

Supplementary Figure 4. Negative regulation of IgA class switching by TBK1. (a,b) Spleen B cells of WT and TBK1-BKO mice (6 weeks old) were cultured in the presence of the indicated inducers: LPS (1 μg/ml), IL-4 (40 ng/ml), anti-CD40 (1 μg/ml), or BAFF (200 ng/ml). Flow cytometry was performed on day 5 to quantify the percentage (numbers in quandrants) of IgA^+ and $IgG1^+$ B cells based on intracellular IgA and IgG1 and surface CD19. Data are representative (**a**) and mean±S.D. values (**b**) of three independent experiments. (**c**) Spleen B cells of WT and TBK1-BKO mice were cultured in the presence of the indicated inducers for 4 days. Real-time quantitative PCR was performed to analyze the relative expression level of Aicda and germ-line transcript (GLT) of IgA (αGLT) and IgG1 (γ1GLT). Data are relative mRNA concentration relative to an internal control β-actin and presented as mean±S.D. values of three independent experiments. *P<0.05 and **P<0.01.

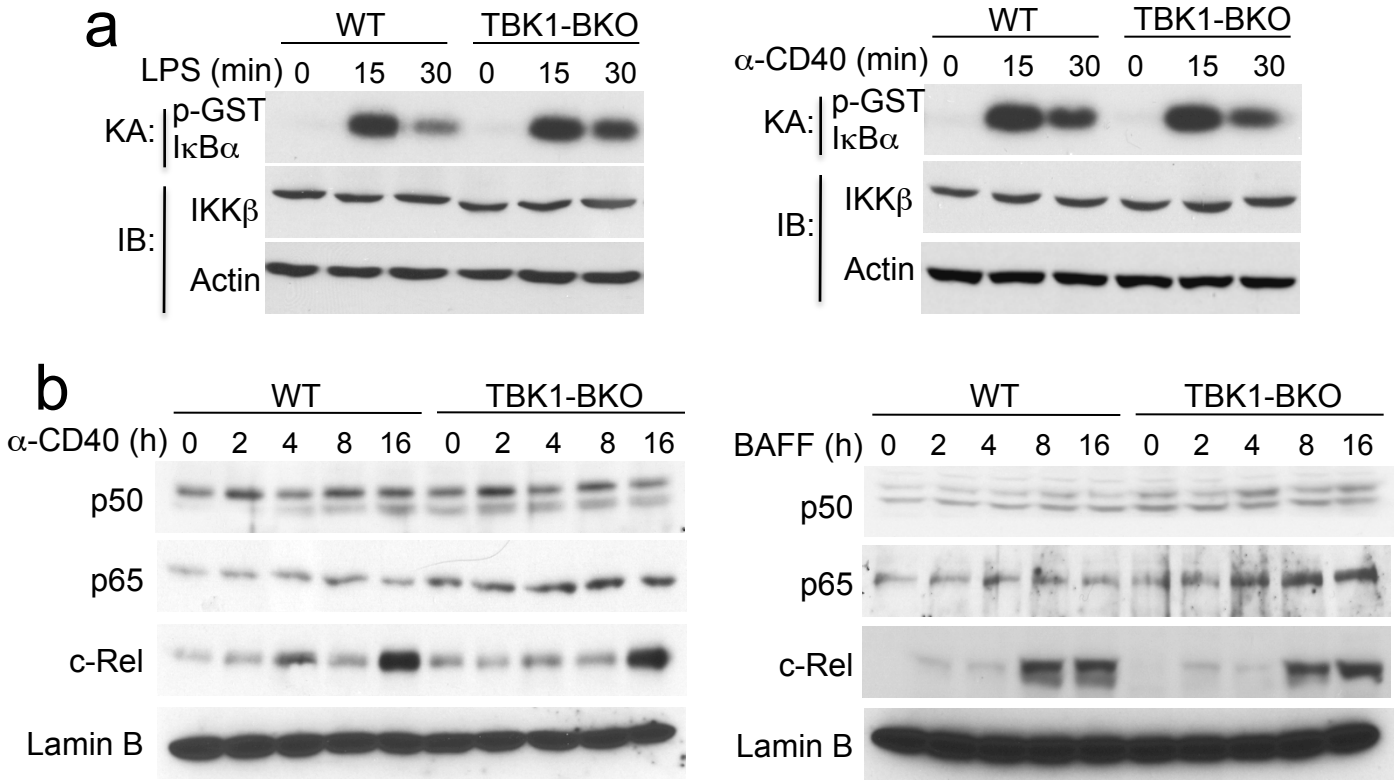

Supplementary Figure 5. TBK1 deficiency does not substantially promote activation of IKK and canonical NF-κB in B cells. Spleen B cells derived from WT and TBK1-BKO mice (6 week old) were stimulated as indicated. (**a**) Kinase assays (KA) detecting IKK activation using GST-IκBα as substrate and parallel IB assays monitoring the expression of IKKβ and loading control Actin. (**b**) IB assays detecting the indicated NF-κB proteins and the loading control Lamin B in the nuclear extracts prepared from the anti-CD40- and BAFF-stimulated WT and TBK1-BKO B cells.

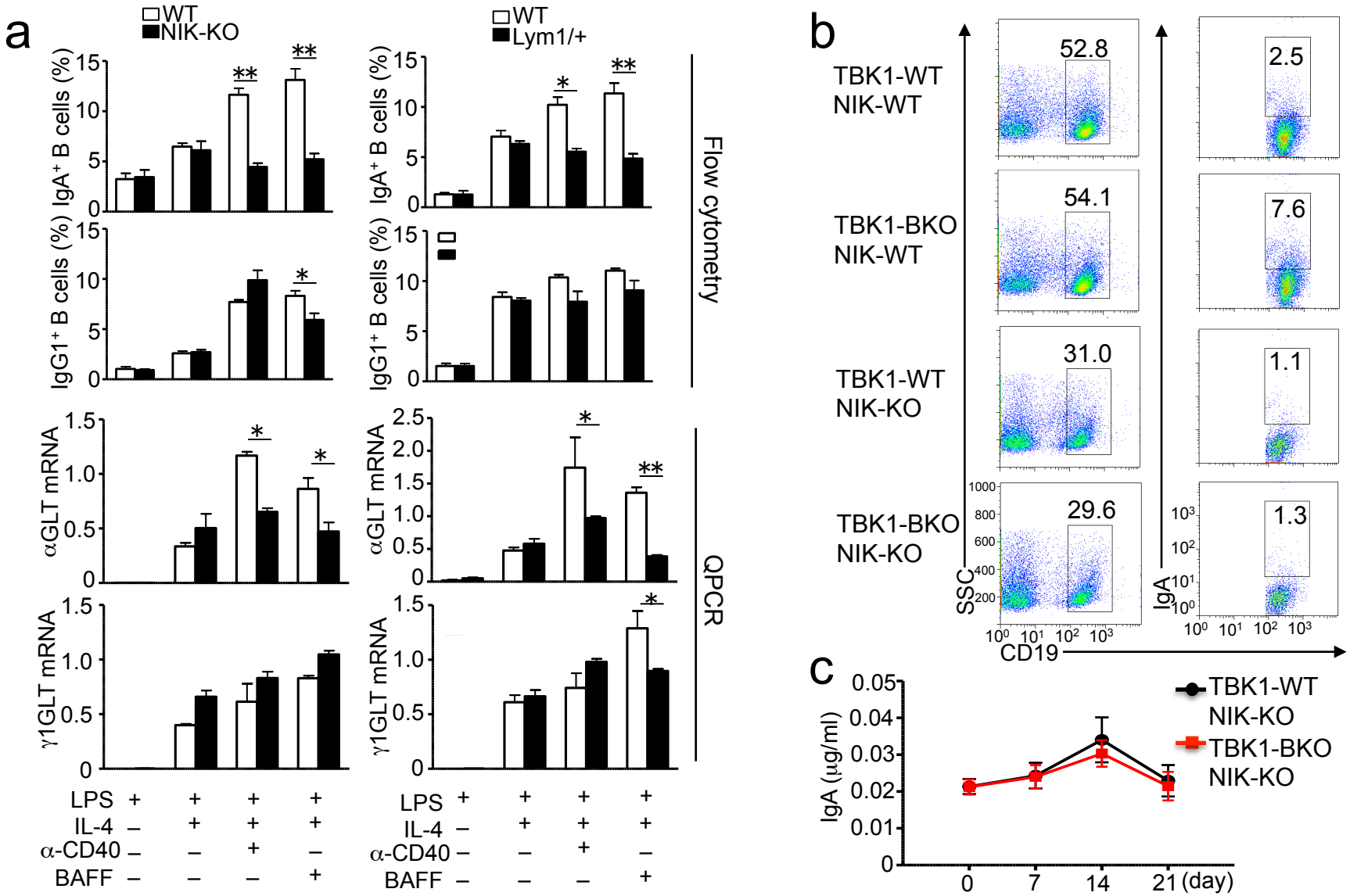

Supplementary Figure 6. Regulation of IgA class switching by NIK and NF-κB2. (**a**) Spleen B cells derived from Map3k14 KO and nfκb2^{Lym1} heterozygous (Lym1/+) mice or their WT control mice were subjected to in vitro class-switching. Flow cytometry and QPCR were performed to quantify the frequency of IgA$^+$ and IgG1$^+$ B cells and the relative mRNA expression of αGLT and γ1GLT. Data are representative of two experiments. *P<0.05 and **P<0.01. **(b)** Frequency of IgA$^+$ B cells (numbers in right panels) in the indicated mice (6 week old) immunized with sheep red blood cells for 7 days. Data are representative of two experiments. **(c)** ELISA of NP-specific IgA in sera of the indicated mice (6 week old) immunized with NP-KLH. Data are presented as mean ±S.D. of three animals and are representative of two experiments.

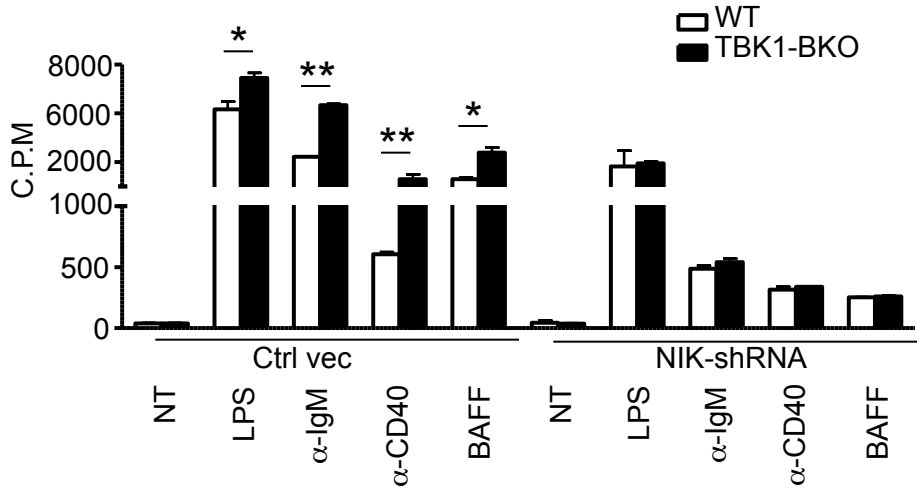

Supplementary Fig. 7. TBK1 deficiency causes increased B-cell proliferation in an NIK-dependent manner. WT and TBK1-BKO B cells were infected with pGIPZ control vector or NIK shRNA. The infected cells were enriched by flow cytometric cell sorting based on GFP expression and then restimulated for 48 h either in the absence (NT) or presence of the indicated inducers: LPS (100 ng/ml), anti-IgM (10 μg/ml), anti-CD40 (1 μg/ml), and BAFF (200 ng/ml). Cell proliferation was measured by thymidine incorporation. Data are presented as mean ±S.D. *P<0.05 and **P<0.01.

Peptide Sequence	Residues
LEAVEK**S**PVFCGK	42–54
DGSEGGPPAISIIAQAECEN**S**QEFSPTFSER	69–99
IFIAGSQQYSQSE**S**LDQIPNNVAHATEGK	100–128
SK**S**LAQAGVALAKPLPR	151–167
VPVEEYLVHALQGSVS**S**GQAH**S**LA**S**LAK	333–360
GEYKEPRPPPQDQATCHQTLP**T**PPR	669–693
APALNL**S**KEESGTWEPLPLSSLDPATAK	722–749
GP**S**FPDRR	750–757
DTL**SS**GVHSWNSQAEAR	817–833
VQIQ**S**LNGEHLHIR	858–871

Supplementary Table 1. Identification of TBK1 phosphorylation sites in NIK by Mass spectrometry. HEK293 cells were co-transfected with plasmids encoding murine NIK and TBK1, and after 48 hrs, the cells were incubated for 2 hours with a proteasome inhibitor, MG132. NIK was isolated from the cell lysates by immunoprecipitation and subjected to mass spectrometry to identify its phosphorylation sites. NIK was also expressed without TBK1 to monitor its autophosphorylation. TBK1-induced NIK phosphorylation sites are shown in red.